DEFENSE TECHNICAL INFORMATION CENTER

Information for the Defense Community

DTIC® has determined on 07/16/2010 that this Technical Document has the Distribution Statement checked below. The current distribution for this document can be found in the DTIC® Technical Report Database.

☒ **DISTRIBUTION STATEMENT A.** Approved for public release; distribution is unlimited.

☐ **© COPYRIGHTED**; U.S. Government or Federal Rights License. All other rights and uses except those permitted by copyright law are reserved by the copyright owner.

☐ **DISTRIBUTION STATEMENT B.** Distribution authorized to U.S. Government agencies only (fill in reason) (date of determination). Other requests for this document shall be referred to (insert controlling DoD office)

☐ **DISTRIBUTION STATEMENT C.** Distribution authorized to U.S. Government Agencies and their contractors (fill in reason) (date of determination). Other requests for this document shall be referred to (insert controlling DoD office)

☐ **DISTRIBUTION STATEMENT D.** Distribution authorized to the Department of Defense and U.S. DoD contractors only (fill in reason) (date of determination). Other requests shall be referred to (insert controlling DoD office).

☐ **DISTRIBUTION STATEMENT E.** Distribution authorized to DoD Components only (fill in reason) (date of determination). Other requests shall be referred to (insert controlling DoD office).

☐ **DISTRIBUTION STATEMENT F.** Further dissemination only as directed by (inserting controlling DoD office) (date of determination) or higher DoD authority.

Distribution Statement F is also used when a document does not contain a distribution statement and no distribution statement can be determined.

☐ **DISTRIBUTION STATEMENT X.** Distribution authorized to U.S. Government Agencies and private individuals or enterprises eligible to obtain export-controlled technical data in accordance with DoDD 5230.25; (date of determination). DoD Controlling Office is (insert controlling DoD office).

Visible lesion thresholds and model predictions for Q-switched 1318-nm and 1540-nm laser exposures to porcine skin

Justin J. Zohner[1], Kurt J. Schuster[1], Lucas J. Chavey[1], David J. Stolarski[1], Semih S. Kumru[2], Benjamin A. Rockwell[2], Robert J. Thomas[2], and Clarence P. Cain[1]

[1]Northrop Grumman, 4241 Woodcock Dr., Ste. B-100, San Antonio, TX 78228-1330
[2]U. S. Air Force, AFRL/HEDO, Brooks City-Base, TX 78235-5278

ABSTRACT

Skin damage thresholds were measured and compared with theoretical predictions using a skin thermal model for near-IR laser pulses at 1318 nm and 1540 nm. For the 1318-nm data, a Q-switched, 50-ns pulse with a spot size of 5 mm was applied to porcine skin and the damage thresholds were determined at 1 hour and 24 hours postexposure using Probit analysis. The same analysis was conducted for a Q-switched, 30-ns pulse at 1540 nm with a spot size of 5 mm. The Yucatan mini-pig was used as the skin model for human skin due to its similarity to pigmented human skin. The ED_{50} for these skin exposures at 24 hours postexposure was 10.5 J/cm^2 for the 1318-nm exposures, and 6.1 J/cm^2 for the 1540-nm exposures. These results were compared to thermal model predictions. We show that the thermal model fails to account for the ED_{50} values observed. A brief discussion of the possible causes of this discrepancy is presented. These thresholds are also compared with previously published skin minimum visible lesion (MVL) thresholds and with the ANSI Standard's MPE for 1318-nm lasers at 50 ns and 1540-nm lasers at 30 ns.

Keywords: laser, skin, near-IR, MVL, safety, LIB

I. INTRODUCTION

Recent developments in solid state and chemical lasers technology have facilitated the growing use of pulsed, high-peak-power lasers at the 1300-nm and 1500-nm wavelengths. Numerous medical, military and industrial applications have been identified. While several ocular injury studies for 1300 and 1500 nm exist, few skin injury studies have been conducted at these wavelengths, especially for Q-switched operation. Prior to the recent advancements in the capability of these laser systems, particularly the in the 1540-nm regime, little concern was given to potential skin hazards associated with these systems. However, higher-energy systems at these wavelengths are becoming available in smaller, more reliable packages. Table-top laser systems are capable of producing microsecond pulses with tens of joules of energy per pulse [1].

This study provides the estimated dose (ED_{50}) required for a 50% probability of producing laser–induced lesions to skin. ED_{50} data for skin injury at 1 hour and 24 hours postexposure were determined for high-energy, Q-switched laser exposures at 1318 nm with pulse duration of 50 ns and beam diameter of 5 mm. In addition, ED_{50} for 1540-nm exposures with pulse duration of 30 ns and beam diameter of 5 mm were determined at 1 hour and 24 hour postexposure. The data were collected using the Yucatan mini-pig (*Sus scrofa domestica*) as the *in vivo* model. The Yucatan mini-pig was selected due to the similarity of its flank skin to that of the human forearm skin. The reported ED_{50} for each wavelength was compared to predicted damage using thermal modeling.

Optical Interactions with Tissue and Cells XVII, edited by Steven L. Jacques, William P. Roach,
Proc. of SPIE Vol. 6084, 60840E, (2006) · 1605-7422/06/$15 · doi: 10.1117/12.644757

II. MATERIALS AND METHODS

For both wavelengths measured, the procedure for obtaining the ED_{50} was essentially the same. Laser exposures at various energies were delivered to the subjects and Probit [2] analysis was used to determine the ED_{50}. The exposures were placed in the spaces of two 6-cm x 6-cm square grids on each flank. The energy was systematically varied over a wide range between maximum and minimum energy delivered. The placement of the energy was in a pseudo-random order determined prior to exposure. The only major differences in the procedure for measuring the ED_{50}s are in the laser used and the slight differences in the optical setup for each laser due to the different methods for varying the exposure energy.

2.1 Animal prep

Yucatan mini-pigs, weighing between 15 and 20 kg, were used as the *in vivo* model in this study. Three separate flanks were used at each wavelength. The study progressed under the animal use protocol titled "Evaluation of Laser induced Corneal Lesions in the Dutch Belted Rabbit and Skin Lesions in the Yucatan Mini-Pig," which was approved by the Brooks City-Base, TX Institutional Animal Care and Use Committee (IACUC). None of the animals were euthanized after exposure or biopsy. The subjects were fed standard diets and had unlimited access to water. However, solid food was withheld for 12 hours prior to laser exposure and biopsy collection. The animals involved in this study were procured, maintained, and used in accordance with the Federal Animal Welfare Act and the "Guide for the Care and Use of Laboratory Animals" prepared by the Institute of Laboratory Animal Resources -- National Research Council. Brooks City-Base, TX has been fully accredited by the Association for Assessment and Accreditation of Laboratory Animal Care, International (AAALAC) since 1967.

The Yucatan mini-pig subjects were received from an attending veterinary technician via stretcher, sedated with an indwelling intravenous catheter placed in an ear vein, and intubated prior to arrival at the laboratory. The pigs were sedated by a single syringe injection of Tiletamine/Zolazepam (4-6 mg/kg) intramuscular (IM) and Xylazine (2.2 mg/kg) IM, and maintained on inhalation isoflurane anesthesia during all procedures. After sedation, hair on the flank was clipped using hand clippers and the underlying skin was cleansed with chlorhexadine solution and allowed to air dry. Prior to the experimental procedures, the cleansed skin was inspected by each of three evaluators to check for redness, irritation or other confounding marks. All subjects were kept warm during the entirety of the procedures. Physiological parameters were monitored throughout all procedures. Buprenorphine (0.05-0.1 mg/kg) was administered intramuscularly for analgesia after biopsies were complete. The animals were returned to their runs upon recovery to sternal recumbency from anesthesia.

2.2 1318-nm exposures

The exposures for the determination of ED_{50} at 1318 nm were delivered using a Nd:YAG, Q-switched laser. The laser produced a single pulse with 50-ns duration. The energy of each pulse was varied by a polarizing, beam-splitting cube and $\lambda/2$ waveplate combination. The cube and waveplate combination were set up inside the laser cavity itself. The delivered energy of a single pulse ranged from ~100 mJ to 3 J. The delivered energy was measured by placing a beamsplitter in the beam path and directing a fraction of the energy onto an energy probe (Molectron JD25 and JD50), and read with an energy meter (Molectron EPM2000). This detector measured what is known as the reference energy. Before and after each exposure set, a second energy probe (Ophir 30[150]-A-HE) was placed at the location of the subject; this detector measured the delivered energy. The ratio between the reference energy and the delivered energy was recorded for each setting of the $\lambda/2$ waveplate used in the exposures (see Figure1).

The desired exposure beam diameter was achieved by placing a telescope consisting of a negative lens followed by a positive lens. The spot size of 5 mm was produced by adjusting the placement of the subject with respect to the final positive lens. A co-aligned argon laser was used as a visible alignment beam to

aim the IR beam onto the subject. A steering mirror was placed after the telescope to make slight adjustments to the vertical and horizontal placement of the alignment beam. The distance between the subject and the final positive lens was kept constant to ensure a consistent beam diameter for each exposure.

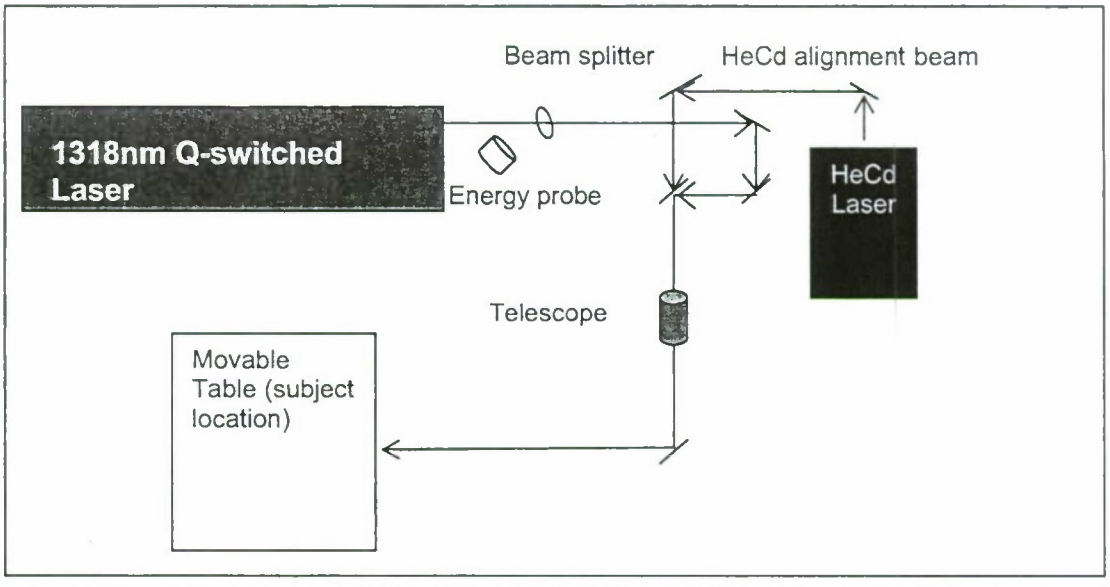

Figure 1. 1318-nm experimental setup. Exposure energy was varied by rotation of a ½-wave plate located within the 1318-nm Q-switched laser.

2.3 1540-nm exposures

A flashlamp-pumped, Er:Glass laser was used to provide the exposures at 1540 nm. The laser produced pulses in the 30-40-ns range at various pulse energies up to 3.5 joules per pulse. The layout of the optical system consisted of a 90/10 beamsplitter followed by a 1-m focal length lens. The lens was used to achieve the desired spot size of 5 mm. A final turning mirror was used to aim the beam to the desired location. Energy measurements of the laser light passing through the beamsplitter were made using an Ophir Laserstar energy meter with Ophir (model number: 30[150]-A-HE) energy probes. A HeNe laser was used as a visible alignment beam to help locate the exposure point (see Figure 2).

As with the 1318-nm exposures, energy measurements were made at the subject location before and after each set of exposures. The ratio of these two energy readings was used to determine the delivered energy for each exposure based on the recorded energy through the beamsplitter. Due to the limited spatial range of the final turning mirror, the position of the subject needed adjusting for some of the exposure locations. A sling was utilized to make the small spatial adjustments. The subject's elevation could be changed as well as the lateral position of the subject. Again, the distance of the subject from the laser was kept constant to ensure uniform spot size for each exposure.

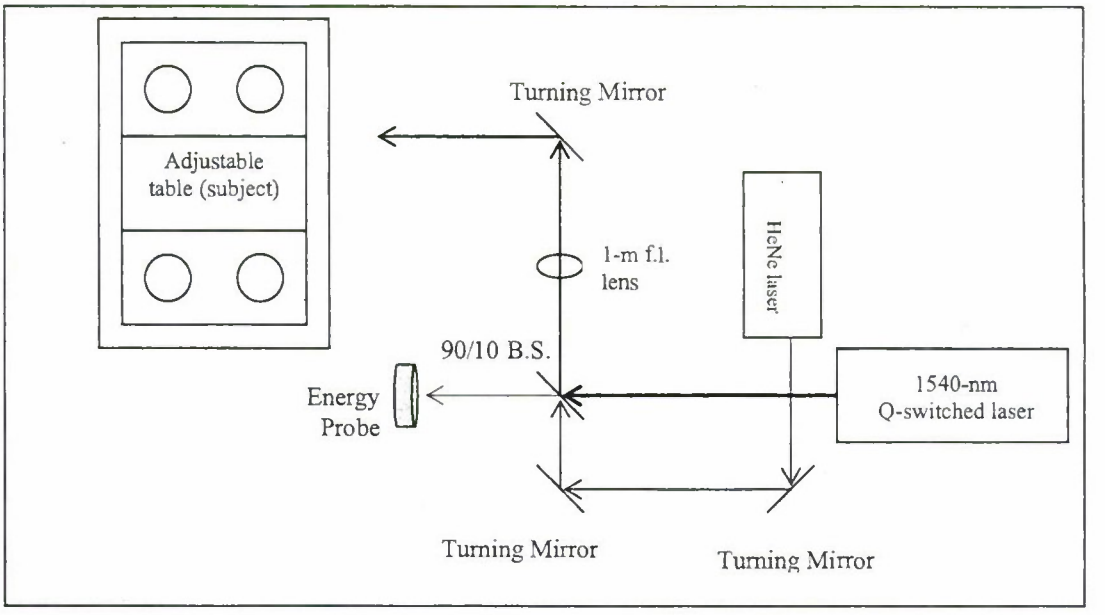

Figure 2: 1540-nm experimental setup. Distance from the 1-meter focal length lens to the subject was kept constant.

2.4 Reading and analysis

During the exposures, notes were made if an exposure caused an audible "pop", a visible flash, or both. The exposures were examined at 1 hour and 24 hours postexposure. Three trained readers independently examined each exposure site and recorded either "lesion" or "no lesion" for each site. Once the three readers were finished, the individual results were compared. Agreement of at least two of the three readers was needed for a positive lesion result to be confirmed.

The Probit[2] statistical analysis package was used to calculate the ED_{50} for each wavelength. Supporting the analyses of the ED_{50}, the fiducial limit at the 95% confidence level, along with the slope and probability of the Probit curve was also calculated at each wavelength at both 1 hour and 24 hours postexposure. Following the experimental exposures, two 5-mm punch biopsies were obtained from each subject immediately after the 1-hour reading and two biopsies again after the 24-hour reading. Biopsies were submitted for complete histological analysis. A control biopsy was collected on a portion of the flank superior to any of the exposure sites. All biopsy sites were closed with non-absorbable 2-0 sutures and topically medicated with Trio-mycin ointment for infection prophylaxis. The results of histological analysis were not available at the time of publication and will be reported in future manuscript

III. RESULTS

The calculated ED_{50} for 1318 nm is based on 216 exposures on three subjects. On each subject 72 exposures were placed on one flank. The 1540-nm ED_{50} was calculated using 216 exposures as well; however, two subjects were used. Both flanks of one subject received 72 exposures and one flank of the other subject was used. Table 1 lists the results for the 1318-nm and 1540-nm exposures at both 1 hour and 24 hours postexposure. Along with the ED_{50}, the slope for each Probit curve is given. The ED_{50}s reported here are above the MPE (maximum permissible exposure) level as set by ANSI (Z136.1-2000)[3] for skin exposures at the reported wavelengths and pulse durations. The MPE for the 1318-nm exposure condition studied here is a value of 0.1 Jcm^{-2}. The MPE for the 1540-nm exposures is 1.0 Jcm^{-2}. The results for the

1540-nm exposures agree reasonably well with other work[4-8] considering the difference in spot sizes and pulse durations.

The majority of the lesions occurred on exposure sites in which an audible "pop" and visible flash were observed. This suggests that the high peak-irradiances incident on the skin induced the formation of a plasma at the interface between the transport medium (air) and the subject medium (skin). This plasma was facilitated by the presence of impurities (i.e. dead skin cells) on the surface of the skin. We will examine the role of this plasma as part of the damage mechanism in the following section.

Experimental Setup Number of Subjects & Exposures	ED_{50} (J cm^{-2}) 1-Hour Reading	ED_{50} (J cm^{-2}) 24-Hour Reading	Probit Curve Slope = δprob/ δdose*
1318 nm 5-mm beam diameter 50 ns Three subjects, three flanks 216 exposures	6.5 (7.0 – 5.9)	10.5 (11.1 – 10.0)	10.7
1540 nm 5-mm beam diameter 30 ns Two subjects, three flanks 216 exposures	6.3 (6.8 – 5.8)	6.1 (6.5 – 5.5)	6.6

* Probit curve slope for 24-hr ED_{50}.

Table 1: 1-hr and 24-hr ED_{50}. Fiducial limits are shown in parentheses.

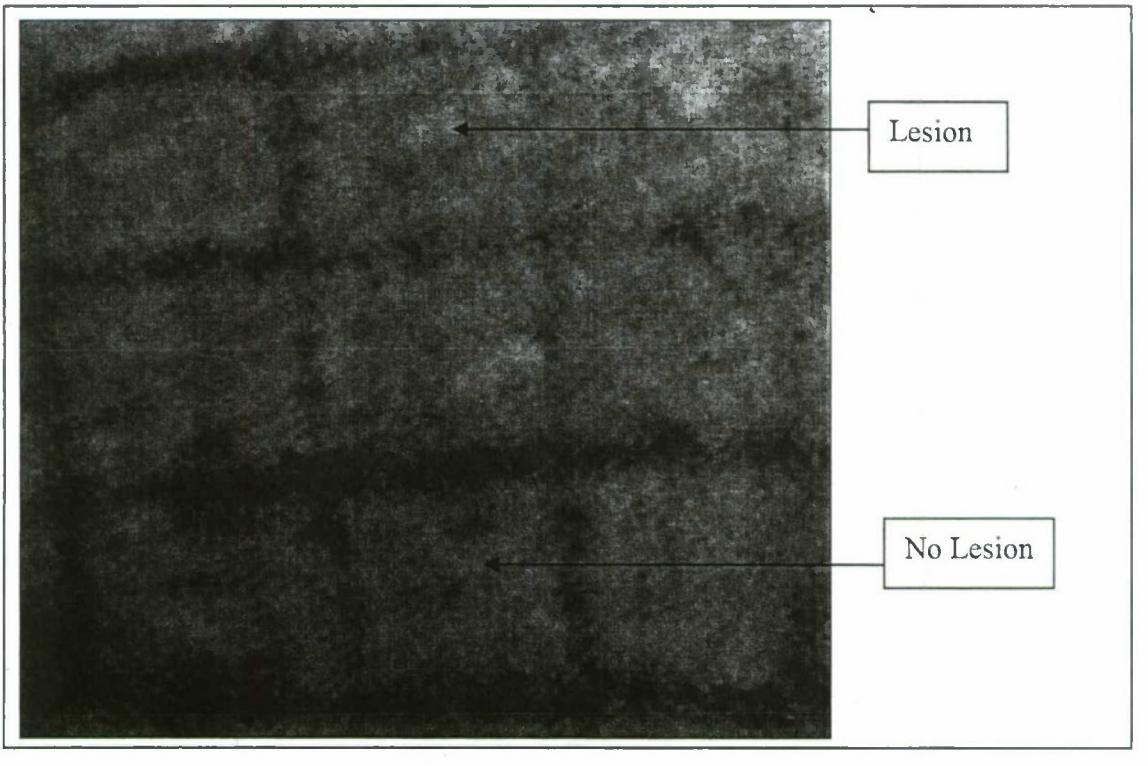

Figure 4: 1318-nm laser exposures after 24 hours, showing slight reddening at lesion site.

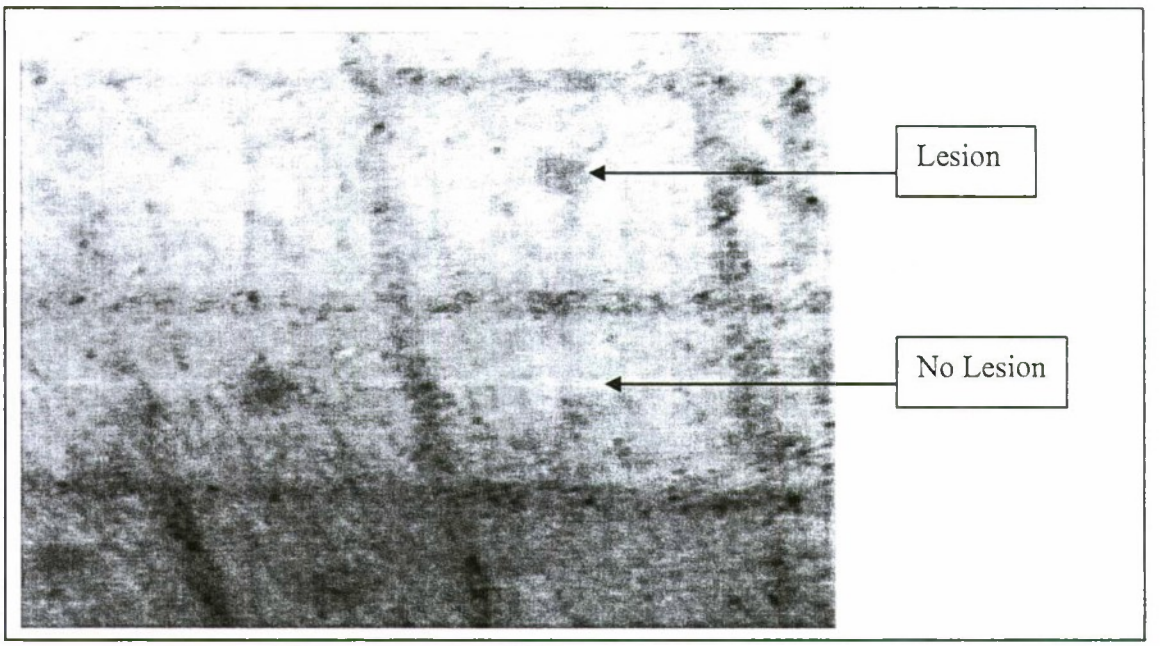

Figure 6: 1540-nm laser exposures after 24 hours, showing lesion site compared to no-lesion site.

IV. DISCUSSION

It is interesting to note the differences in the 1-hr and 24-hr ED_{50}s for the two wavelengths. For the 1318-nm exposures, the ED_{50} threshold increases from the 1-hr to the 24-hr exposures. This may indicate the type of damage incurred by the tissue. It appeared that most of the 1-hr lesions were on the surface of the skin. The lesions were generally white in color and did not seem to raise the skin in a significant manner. Many of these lesions were no longer visible at 24 hrs, suggesting that only the outermost layer of the skin was affected. This could possibly be due to the pulse duration (50 ns) and high peak-irradiances used for these exposures. However, the thresholds for the 1-hr and 24-hr ED_{50}s for the 1540-nm exposures remained virtually constant. The spot sizes used were comparable, as were the pulse durations (30ns) and peak irradiances. This may suggest a wavelength-dependent effect as to why the lesions produced by exposure to 1540-nm laser light possessed a higher probability of being visible at 24 hrs post exposure. The lesions observed at 1 hr for the1540-nm exposures were much redder in color and raised the skin in a blistering fashion. In addition, some of the lesions produced with the 1540-nm laser, particularly those produced using the maximum radiant exposure, persisted for several weeks, as seen in the small brown spots in Figure 7.

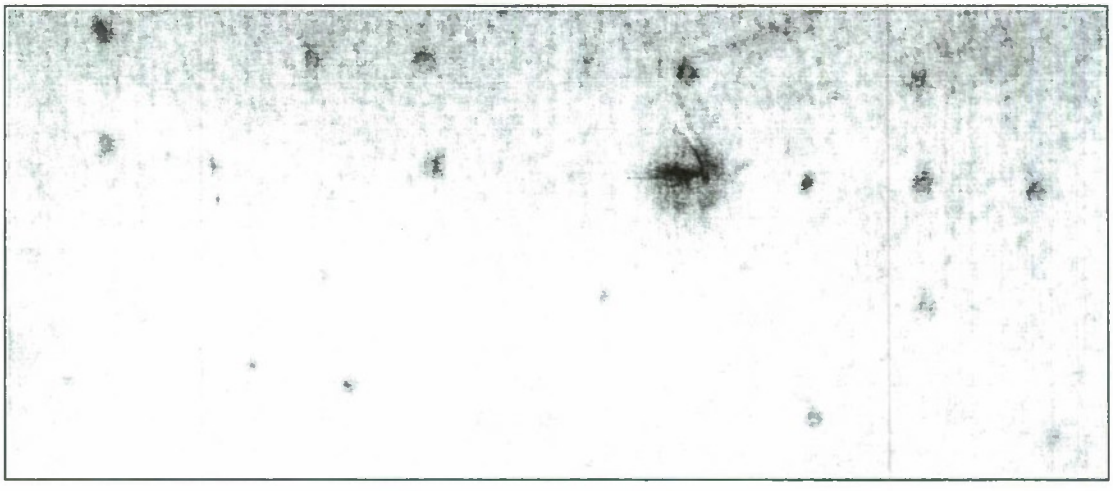

Figure 7: 1540-nm laser exposures after 2 weeks. The dark scar with sutures is a biopsy punch site.

4.1 Thermal damage modeling

At the wavelengths studied, the normal damage mechanism for long pulses and continuous wave exposures is photothermal. However, at the pulse durations and energy levels reported in this study, the exposures are within the thermal confinement regime[9], suggesting that thermal damage of the tissue is unlikely. To accomplish this task, thermal damage models were used to compare computational predictions at infrared wavelengths to physical data. The thermal damage model used in this work is a modified version of the work done by Henriques[10]. The damage model takes the basic form of a rate equation for heat transfer:

$$\Omega(r,z) = A\int_0^t \exp(-E/RT)dt \qquad (1)$$

where

A = pre-exponential factor (s^{-1})
E = activation energy for the reaction (cal/M)
R = 2.0 = universal gas constant (cal/M·K)
$T = T(r,z,t)$ temperature (K)
$\Omega(r,z)$ = damage integral
t = time at final recovery of temperature after exposure.

Henriques set up the rate equation such that complete necrosis of affected skin cells occurs when $\Omega = 1$. From this condition the values for A and E are found to be:

$A = 3.1 \text{ X } 10^{98}$ (1/s)
E = 150,000 (cal/M).

The Takata Model[11] used in this study solves Eq. (1) by employing a "finite difference" method used by Mainster, *et al.*[12, 13] It also introduces modifications to take into account specific skin geometries as well as optical and thermal properties of the skin. Additionally, the Takata model allows for appropriate alteration of the beam profile as the beam passes through various layers of skin.

Calculations for each wavelength were conducted to estimate the temperature rise caused by the laser exposure. The calculated temperature rises were then compared to the minimum visible lesion (MVL) threshold associated with temperature rises of skin. The results suggest that the mechanism for the damage observed from these laser exposures is not exclusively thermal in nature. The predicted temperature rise

for the laser exposures at 1318 nm were 4° C without modeling intercellular scattering and 8° C when the scattering was included. This is quite low compared to the 2nd-degree burn MVL threshold of ~29°C. The results were similar for the 1540-nm exposures. A temperature rise of 4.7°C was calculated through the model, which again is lower than the thermal ED_{50} of 29°C.

4.2 Plasma formation

The model used obviously does not account for the damage produced by these laser exposures. While the pulse duration and energy levels observed at the reported ED_{50} levels are within the stress confinement criteria[9], the damage mechanism responsible for the lesions is not thought to be ablative in nature. The ED_{50} levels reported here appear to be well below the extrapolated thresholds determined from results of nanosecond pulses at 1064 nm.[14] As mentioned above, no histological results are available at time of printing and these results will allow a definitive answer on whether or not ablation was occurring due to the exposures.

Although the ED_{50} levels reported here seem to be below the thresholds for tissue ablation, the levels are capable of inducing a laser induced breakdown (LIB) event at the skin's surface. The ED_{50} for both wavelengths correspond to roughly $2x10^8$ W/cm^2 ($2.1x10^8$ W/cm^2 for 1318-nm pulses, and $2.03x10^8$ W/cm^2 for 1540-nm pulses). These irradiance levels lie within the plasma formation threshold for short laser pulses described in Welch[9]. Using an index of refraction[15] for the skin of n=1.4, the electric field due the laser pulse impinging on the skin for both wavelengths is ~$3.3x10^7$ V/m.[16] This result confirms the flashes of white light noted during exposures at and above the ED_{50} level were due to LIB. This also explains the acoustic "pop" heard during the exposures.

As mention above, the 1318-nm and 1540-nm exposures are in the stress confinement regime. This suggests that the shock wave created by the acoustic pop is capable of causing mechanical damage to the skin. Additionally, the plasma itself may cause surface temperatures of the skin to rise much higher than the thermal model used predicts. Plasma clouds of this nature can reach temperatures of several thousand degrees K.[16] The short time-scales and high peak-irradiances involved with these laser exposures are not characterized well with existing thermal models employed in this work.

V. CONCLUSIONS

ED_{50} data are reported for the wavelengths of 1318 nm and 1540 nm with pulse durations of 50 ns and 30 ns respectively. Beam diameters of 5 mm where used for both wavelengths studied. The data reported are compared to ANSI Z136.1-2000 and found to be above the listed MPE for each case. Thermal modeling analysis is also conducted and a discrepancy is found between the model predictions of temperature rise and observed ED_{50}s. The predicted temperature rise from the model is much lower than the 2nd-degree burn threshold. Perhaps the thermal rise of the skin is greater than the thermal model predicts due to the short time scale involved. Moreover, the plasma created during the exposure may have caused heating of the tissue that the model does not take into account. Another possibility is that the acoustic wave created by the formation of the plasma caused the damage. More work in the modeling of interactions between laser radiation and *in vivo* subjects needs to be conducted for situations with similar time scales and peak irradiances.

REFERENCES

1 J. Taboada, J. M. Taboada, D. J. Stolarski, J. J. Zohner, L. J. Chavey, H. Hodnett, G. D. Noojin, R. J. Thomas, C. P. Cain, and S. S. Kumru, "100-megawatt Q-switched Er:glass laser," *SPIE Proceedings*, 2006.

2 D. J. Finney, *Probit Analysis*, 3rd ed. New York, NY: Cambridge University Press, 1971.

3 ANSI, "Z136.1 American National Standard for Safe Use of Lasers." Orlando, Florida: Laser Institute of America, 2000.
4 C. P. Cain, G. Polhamus, W. P. Roach, D. J. Stolarski, K. J. Schuster, K. Stockton, B. A. Rockwell, B. Chen, and A. J. Welch, "Porcine skin visible lesion thresholds for near-IR lasers, including modeling, at two pulse durations and wavelengths," *Journal of Biomedical Optics*, 2006.
5 A. V. Lukashev, B. I. Denker, P. P. Pashinin, and S. E. Solovyev, "Laser Damage of Skin by 1540 nm Er-glass Laser Radiation. Impact to Laser Safety Standards," *Proceedings of SPIE*, vol. 2965, pp. 22-32, 1996.
6 A. V. Lukashev, S. E. Sverchov, V. P. Solovyev, B. I. Denker, V. V. Engovatov, and P. P. Pashinin, "Investigation of laser damage on skin by 1540 nm Er-glass laser," General Physics Institute, Russian Academy of Sciences, Moscow, Technical Report 16 September 1995 1995.
7 P. J. Rico, M. A. Mitchell, T. E. Johnson, and W. P. Roach, "ED50 Determination and Histological Characterization of Porcine Dermal Lesions Produced by 1540 nm Laser Radiation Pulses," presented at Lasers in Surgery: Advanced Characterization, Therapeutics, and Systems X, San Jose, CA, 2000.
8 P. J. Rico, T. E. Johnson, M. A. Mitchell, B. H. Saladino, and W. P. Roach, "Median Effective Dose Determination and Histologic Characterization of Porcine (Sus scrofa domestica) Dermal Lesions Induced by 1540-nm Laser Radiation Pulses," *Comparative Medicine*, vol. 50, pp. 633 - 638, 2000.
9 A. J. Welch and M. Van Gemert, *Thermal Response of Tissue to Optical Radiation*. New York: Plenum Press, 1995.
10 F. F. Henriques, "Studies of thermal injury," *Archives Of Pathology*, vol. 43, pp. 489, 1947.
11 A. N. Takata, D. Zaneveld, and M. S. Richter, "SAM-TR-77-38 Laser Induced Thermal Damage of Skin," USAF School of Aerospace Medicine, Brooks Air Force Base, TX, USAF Technical Report SAM-TR-77-38, 1977 1977.
12 M. A. Mainster, T. J. White, and R. G. Allen, "Spectral Dependence of Retinal Damage Produced by Intense Light Sources," *Journal of the Optical Society of America*, vol. 60, pp. 848, 1970.
13 M. A. Mainster, T. J. White, J. H. Tips, and P. W. Wilson, "Transient Thermal Behavior in Biological Systems," *Bulletin of Math Biophysics*, vol. 32, pp. 303-314, 1970.
14 X.-H. Hu, Q. Fang, M. Cariveau, X. Pan, and G. W. Kalmus, "Mechanism study of porcine skin ablation by nanosecond laser pulses at 1064, 532, 266, and 213 nm," *IEEE Journal of Quantum Electronics*, vol. 37, pp. 322-328, 2001.
15 J. G. Fujimoto, S. D. Silvestri, E. P. Ippen, C. A. Puliafito, R. Margolis, and A. Oseroff, "Femtosecond optical ranging in biological systems," *Optics Letters*, vol. 11, pp. 150-152, 1986.
16 P. R. Willmott and J. R. Huber, "Pulsed laser vaporization and deposition," *Reviews of Modern Physics*, vol. 72, pp. 315-328, 2000.